Morphology and magnetism of Fe_n clusters ($n=1-9$) supported on a Pd(001) substrate

Jürgen Hafner* and Daniel Spišák

Fakultät für Physik and Center for Computational Materials Science, Universität Wien, Sensengasse 8, A-1090 Wien, Austria

(Received 3 May 2007; revised manuscript received 12 July 2007; published 26 September 2007)

We present a detailed *ab initio* density-functional study of the morphology and magnetic and electronic properties of small Fe_n ($n=1-6,9$) clusters and Fe monolayers supported on a Pd(001) substrate. Our focus is on the variation of the cluster moments with the size and shape of the cluster and on the induced magnetization of the substrate. For the smallest clusters, the magnetic moments of the Fe atoms are strongly enhanced compared to bulk Fe. With increasing size of the cluster, the moment decreases linearly with the number of Fe nearest neighbors. The magnetic moment of the adsorbed cluster induces a substantial magnetization of the substrate. The induced magnetic moments are largest on the Pd atoms binding to the cluster atoms, increasing with the number of Fe neighbors. The induced magnetic polarization is quite long ranged, and the enhanced magnetic moments of the Fe atoms and the induced magnetization of the substrate add up to a "giant effective moment" per Fe atom ranging between 7.6 μ_B for an isolated adatom and 4.6 μ_B for a nine-atom cluster. Relaxation of the cluster structure reduces the Fe moments but enhances the induced moments. Orbital moments induced by spin-orbit coupling have been determined via self-consistent relativistic calculations for an isolated Fe adatom. Due to the strong hybridization, the orbital moment on the Fe atom remains rather modest, but a much higher ratio of orbital and spin moments is found for the Pd atoms of the substrate. Relativistic effects also lead to a substantial anisotropy of the induced spin and orbital moments, which makes a significant contribution to the magnetic anisotropy energy.

DOI: 10.1103/PhysRevB.76.094420 PACS number(s): 36.40.Cg, 75.50.Bb, 73.22.−f, 81.07.−b

I. INTRODUCTION

Small metallic clusters supported on or embedded in surfaces represent an interesting and timely field of research. Potential applications of supported metallic clusters range from catalysis to magnetic and magneto-optic storage technologies, exploiting the increased chemical reactivities of nanosized clusters supported on oxides or other nonmetallic substrates and the enhanced magnetism of metal-supported clusters, respectively. However, while for gas-phase clusters, Stern-Gerlach experiments on mass-selected cluster beams[1,2] allow a rather precise determination of the magnetic moment of the superparamagnetic clusters and its variation with the cluster size, similar measurements on supported clusters turned out to be much more difficult. Lau *et al.*[3] have used x-ray magnetic circular dichroism (XCMD) to investigate the size-dependent magnetism of small Fe_n clusters ($n=1-9$) deposited on ultrathin nickel films grown on a Cu(001) substrate. Their results demonstrate that, in general, both spin and orbital moments are enhanced over their bulk values (and also larger than in ultrathin iron films), but it is rather intriguing that both the spin and the orbital components show a nonmonotonous variation with cluster size. This lead the authors to speculate that, due to symmetry, clusters with an odd number of atoms show a different geometric arrangement and, consequently, different magnetic properties than even-numbered clusters. Their findings stand in marked contrast to XCMD studies of Co nanoparticles on Pt(111) by Gambardella *et al.*,[4] where a steady decrease of the magnetic moments with increasing cluster size was reported. Gambardella *et al.* also pointed out that for a highly polarizable substrate such as Pt, the induced magnetic moments of the substrate atoms make a non-negligible contribution to the total measured magnetization. "Giant effective moments" for dilute alloys of Fe in Pd of up to 12 μ_B/Fe atom (of which about 8 μ_B are distributed among the Pd atoms surrounding an Fe impurity) have previously been reported by many groups.[5–8] Ulmeanu *et al.*[9] have used electron paramagnetic resonance to determine the ratio of orbital-to-spin magnetic moments in Fe-Pt nanoparticles and found values of $M_L^{eff}/M_S^{eff} \sim 0.05$ comparable to those for bulk Fe. In a more recent work of the same group,[10] a dramatic increase of the ratio M_L^{eff}/M_S^{eff} of the Fe-Pt nanoparticles upon annealing (leading to the formation of an ordered phase) has been reported—this highlights the pronounced influence of the Fe-Pt coordination on the formation of spin-orbit induced magnetic moments.

The magnetism of supported clusters has been studied theoretically for some time[11–27] at various levels of theory, ranging from semiempirical tight-binding methods[11–15] to fully self-consistent density-functional calculations [most of them based on Green's-function Kohn-Korringa-Rostocker (KKR) methods],[16–27] eventually even including spin-orbit coupling.[14,21,22,27] The results of the recent investigations of Fe clusters on Ni and Cu substrates by Mavropoulos *et al.*[26] are prototypical for these studies: The average spin moments of the clusters are reduced with cluster size, because a higher Fe-Fe coordination increases the hybridization of the *d* states. Measured as a function of the number of Fe neighbors, the local magnetic moment decreases linearly. Rather large differences exist in the prediction of the spin-orbit induced orbital magnetic moments based on tight-binding[14] and on Green's-function KKR methods.[21,22,27] The fully relativistic calculations of Lazarovits *et al.*[22] and of Sipr *et al.*[27] indicate a strong variation of the orbital moment with the substrate and that the size dependence of the orbital moment is even more pronounced than that of the spin moment.

An assumption shared by virtually all of these studies is that the clusters propagate the crystalline structure of the

substrate. If a relaxation of the cluster was considered at all, then it was restricted to the variation of the interlayer distance between the flat cluster and the equally flat surface layer, while the lateral coordinates of the cluster atoms remained in registry with the substrate. Since the lattice constants of the most frequently used substrates (Cu, Ag, Ni, Pd, and Pt) are significantly larger than those of the ferromagnetic 3*d* metals, this means that the bonds between the atoms in such a cluster are under considerable tensile strain. A notable exception is the work of Pick *et al.*[23,24] were a three-dimensional relaxation of small Co clusters supported on and embedded in Cu(001) surfaces has been performed. It was concluded that, despite the relatively small mismatch between Cu and Co, the strain relaxations have a profound influence on the geometry of both cluster and substrate and on the magnetic properties. However, in this case, the relaxation has been calculated using a set of interatomic potentials formulated in a second-moment tight-binding approximation and fitted to total-energy calculations of the bulk substrate material and of single and paired impurities of the cluster atoms in the host. While this is a reasonable first approximation, it is evident that this approach does not account for the many-body character of the interatomic interactions and for their variation with the magnetic state of the cluster atoms.

Studies of the formation of induced moments require a self-consistent calculation of the local spin-polarized density of states for both cluster and substrate atoms—such studies are rather scarce. Sipr *et al.*[27] have calculated the spin moments induced by Co clusters on Pt(111) and Au(111) substrates. The calculations have been performed for a geometry continuing the crystal structure of the substrate and are restricted to nearest neighbors of cluster atoms. Modest spin moments of about 0.1 μ_B are reported. This result stands in marked contrast to the tight-binding study of Co clusters on Pt(111) of Félix-Medina *et al.*[11] reporting induced moments ranging between 0.4 and 0.5 μ_B and to the *ab initio* density-functional study of Dennler *et al.*[28] on Co-doped Rh(111) surfaces reporting induced moments increasing up to 0.6 μ_B with the number of Co neighbors and extending also to more distant neighbors. Effective magnetic moments per Co atom of up to 4 μ_B are calculated. The calculations of the effective magnetization of clusters supported on the surface of 4*d* and 5*d* metals remain a challenge.

Our studies on freestanding and supported magnetic monowires and monolayers[29–32] have demonstrated that not only the magnetic properties of nanostructures change appreciably under applied strain, but also the magnetic ordering may profoundly influence the geometric properties of the nanostructures. For example, the Fe-Rh interlayer distance of an Fe/Rh(001) monolayer is 1.59/1.68/1.78 Å for nonmagnetic, antiferromagnetic, and ferromagnetic Fe layers (to be compared with 1.93 Å in bulk Rh).[32] For freestanding straight Fe monowires, the equilibrium interatomic distance is 1.94 Å for a nonmagnetic, 2.25 Å for a ferromagnetic (magnetic moment of 3.34 μ_B), and 2.38 Å for an antiferromagnetic wire (magnetic moment of ±3.05 μ_B).[29] If the ferromagnetic Fe wire is constrained to match the distances between the binding sites along the edges of a stepped Cu(11*n*), $n=7,9,11$, surface (Fe-Fe distance of 2.57 Å), the magnetic moment is reduced to 3.0 μ_B—in this case not due to an imposed strain but because of the hybridization of the *d* states with the substrate orbitals.

In this paper, we present *ab initio* spin-polarized density-functional investigations of Fe_n nanoclusters on a Pd(001) substrate, i.e., on a system with a substantial size mismatch, based on an unconstrained relaxation of the cluster structure. We concentrate on (i) the geometric structure of the cluster and the adsorption-induced distortions of the substrate, (ii) the dependence of the magnetic properties on the size and geometry of the cluster, and (iii) the contribution of the induced magnetic moments of the substrate atoms to the total magnetization of the cluster-substrate complex. In addition, the contribution of orbital moments to the magnetism of adatoms and substrate is examined by performing self-consistent fully relativistic calculations for an isolated adatom.

II. COMPUTATIONAL METHOD

The quantum-mechanical framework of our investigation is density-functional theory within the local density approximation. The calculations performed in this study have been performed using the VASP (Vienna *ab initio* simulation program) code.[33] This program performs an iterative solution of the Kohn-Sham equations for periodic boundary conditions. The electronic orbitals are expanded in terms of plane waves with a maximal kinetic energy of 280 eV. The electron-ion interaction is described by projector-augmented wave (PAW) potentials.[34,35] The PAW approach shares the computational efficiency of the pseudopotential approach but is an all-electron technique avoiding the problems related to the linearization of the core-valence exchange interaction (this is particularly important for magnetic calculations).

The calculations have been performed in a scalar relativistic mode. The formation of spin-orbit induced orbital moments and their anisotropy have been examined by performing self-consistent fully relativistic calculations. These calculations use an unconstrained vector-field description of the magnetization density and of the exchange field[36,37] and allow, in principle, for a noncollinear orientation of spin and orbital moments. The vector field of the spin and orbital magnetization densities do not necessarily have the symmetry of the crystal lattice; hence, Brillouin-zone integrations have to be performed on the full zone and require in addition a fine *k*-point mesh. The computational effort is further increased by a rather slow convergence of the magnetization directions. Because of the high computational effort required for these calculations, they have been restricted to the case of an isolated Fe adatom.

We use the gradient-corrected exchange-correlation functional proposed by Perdew-Burke-Ernzerhof[38] (PBE) and the spin interpolation of Vosko *et al.*[39] The use of the generalized-gradient approximation is essential for a correct description of the structural and magnetic ground state of Fe.[40] Using the PBE functional, we calculate for face-centered-cubic (fcc) Pd a lattice parameter of $a_{fcc}=3.952$ Å (atomic volume $\Omega=15.430$ Å^3) and a bulk modulus $B=1.66$ Mbar, and for body-centered-cubic (bcc) ferromagnetic Fe lattice parameter of $a_{bcc}=2.828$ Å (atomic volume $\Omega=11.302$ Å^3), a bulk modulus $B=1.66$ Mbar, and a mag-

TABLE I. Point-group symmetry, magnetic cluster moments M_{Fe}, induced moments in the substrate M_{Pd}, and total effective magnetic moment (calculated as the sum of the magnetic moments on the Fe atoms and of the magnetic moments on the Pd atoms), M_{eff} (all per Fe atom), average vertical distances between the nearly planar Fe cluster and the top layer of the Pd(001) surface, $d_{Fe\text{-}Pd}$, average distance between the two top layers in the Pd substrate, $d_{Pd\text{-}Pd}$, average bond length in the cluster, $b_{Fe\text{-}Fe}$, and buckling amplitudes of the cluster and the top layer of the substrate, Δd_{Fe} and Δd_{Pd}, for Fe_n clusters and an Fe monolayer (ML) on Pd(001).

n	Symmetry	M_{Fe} (μ_B)	M_{Pd} (μ_B)	M_{eff} (μ_B)	$d_{Fe\text{-}Pd}$ (Å)	$d_{Pd\text{-}Pd}$ (Å)	$b_{Fe\text{-}Fe}$ (Å)	Δd_{Fe} (Å)	Δd_{Pd} (Å)
1	C_1	3.38	4.26	7.64	1.33	1.95			0.063
2	C_{2v}	3.32	2.95	6.27	1.40	1.96	2.73	0.000	0.084
3	C_{2v}	3.29	2.33	5.62	1.45	1.97	2.73	0.029	0.079
4	C_{4v}	3.22	1.72	4.94	1.52	1.98	2.67	0.000	0.097
5	C_1	3.23	1.77	5.00	1.51	1.99	2.69	0.131	0.106
6	C_{2v}	3.19	1.53	4.72	1.57	1.99	2.66	0.094	0.094
9	C_{4v}	3.18	1.40	4.58	1.58	2.01	2.68	0.214	0.191
ML		3.12	0.56	3.68	1.70	2.06	2.79		

netic moment of $M=2.32\ \mu_B$. The corresponding experimental values are, for Pd, $a=3.96$ Å and $B=1.9$ Mbar and, for bcc Fe, $a=2.867$ Å, $B=1.68$ Mbar, and $M=2.22\ \mu_B$ (Ref. 41).

The Fe_n/Pd(001) system has been modeled by slabs consisting of four Pd layers with a (5×5) unit cell and a sufficiently thick vacuum space of 19 Å. VASP allows us to calculate the Hellmann-Feynman forces acting on ions; hence, a full structural optimization of the cluster-substrate complex may be carried out. During the relaxation, the two bottom layers of the substrate were frozen in a bulklike geometry. The structural relaxation is completed after all forces, except those acting on atoms in the two frozen layers at the bottom of the slab, drop below 10 meV/Å. Brillouin-zone integrations have been performed via the Methfessel-Paxton technique[42] on a $3\times3\times1$ k-point grid and with a smearing parameter of 0.2 eV. All total energies were extrapolated to zero smearing.

Compared to Green's-function KKR calculations modeling adsorbed clusters on a semi-infinite substrate, the advantage of our supercell approach is that it achieves electronic self-consistency for all atoms (which is important for the determination of the induced magnetization), uses the full potential, and allows for a full three-dimensional relaxation of the cluster-substrate complex using the exact Hellmann-Feynman forces. On the other hand, due to the finite size of the supercell, it cannot be avoided that the magnetization clouds induced by periodically repeated larger clusters overlap at the cell boundary. The alternative approach based on the Green's function of the semi-infinite substrate treats the adsorbed cluster plus a part of the vacuum region and of the substrate in contact with the cluster as a perturbation, and the Green's function of the cluster-substrate complex is obtained self-consistently by solving a Dyson equation. For the potential, an atomic-sphere approximation is used and the central region for which a self-consistent solution is constructed contains between 37 and 87 atomic spheres (cluster, substrate, and vacuum).[22,27] Hence, this region contains fewer atoms than our supercell. In addition, no geometric relaxation is permitted. Hence, cluster and Green's-function approaches should be considered as offering complementary information.

III. RESULTS

The growth of Fe clusters and thin films on Pd(001) has been investigated experimentally by various techniques. In the submonolayer regime, Bader and co-workers[43,44] (using Auger and photoemission spectroscopies) and Jin *et al.*[45] (using reflection high energy electron diffraction and scanning tunneling microscopy) report the formation on small randomly distributed islands of monolayer height. With increasing coverage, Boeglin *et al.*[46] and Lee *et al.*[47] report a tendency toward alloying at the interface.

In the following, we describe our results for the structural, magnetic, and electronic properties of Fe_n clusters on Pd(001). As suggested by the experimental studies, we have concentrated our attention on flat clusters with monolayer height. To create a reference, we have also studied a complete Fe monolayer on the same substrate, but intermixing has not been considered. Table I summarizes the results for the symmetry, the average magnetic moments of the Fe atoms and induced in the substrate, and also the main parameters characterizing the geometric structure. Figure 1 shows the relaxed cluster structures; magnetic moments are listed for the Fe atoms in the cluster and for all atoms in the substrate having at least one Fe nearest neighbor. The magnetic moments of the Fe atoms are found to be strongly enhanced, not only compared to the value in bulk bcc Fe ($M_{bulk}=2.32\ \mu_B$) but also compared to the moment in a complete Fe monolayer adsorbed on Pd(001) ($M_{mono}=3.12\ \mu_B$). Substantial magnetic moments are induced in the substrate. On the Pd atoms binding to the cluster atoms, these moments vary between 0.18 and 0.41 μ_B. The induced magnetization is rather long ranged. Together, the effective magnetic moment per Fe atom exceeds by far the limiting value for the spin moment of an Fe atom set by Hund's rule.

A. Geometry and energetics of the cluster-substrate complex

As a consequence of the size mismatch between the nearest-neighbor distances in bulk Pd and Fe of 12%, the

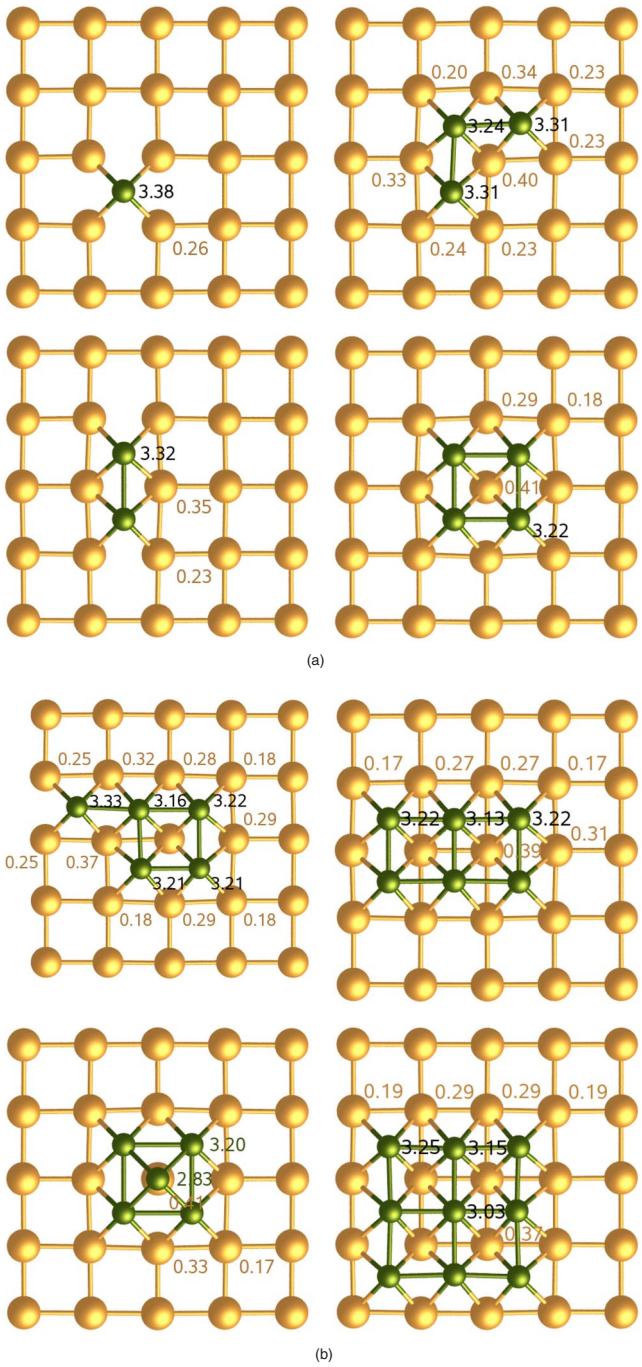

FIG. 1. (Color online) Relaxed structures and magnetic moments of Fe_n clusters with $n=1-6$ and $n=9$ on a Pd(001) surface. The numbers quote the magnetic moments (in μ_B) of the Fe atoms and induced on the Pd atoms of the substrate. For the Fe_5 cluster, a planar and a pyramidal configuration are shown (cf. text).

cluster geometry is quite strongly affected by the relaxation, see Fig. 2. On the clean (001) surface of Pd, the top layer undergoes a slight inward relaxation by −1.2%, compared to an interlayer distance of 1.976 Å in bulk Pd. The most favorable position for the adsorption of an isolated Fe atom on this surface is in a fourfold hollow, at a vertical distance of $d_{\text{Fe-Pd}}=1.326$ Å, which is considerably shorter than the interlayer distance of $d_{\text{Pd-Pd}}=1.976$ Å, and the magnetic moment

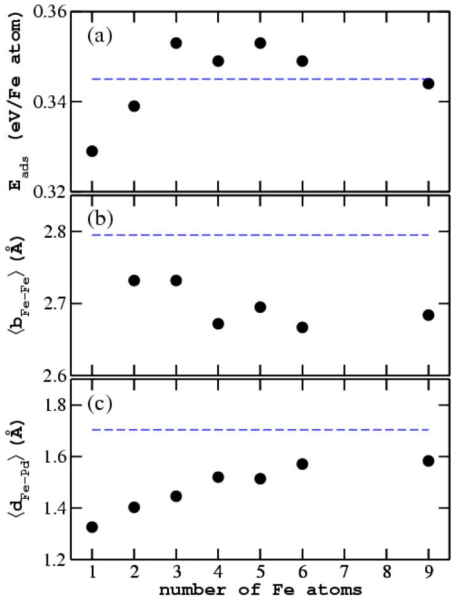

FIG. 2. (Color online) Adsorption energies E_{ads}, average Fe-Fe distance $b_{\text{Fe-Fe}}$ in the cluster, and average distance $d_{\text{Fe-Pd}}$ between the Fe layer and the Pd surface as a function of cluster size. The dashed lines represent the corresponding results for a compact Fe monolayer on Pd(001).

of the Fe atom is $M_{\text{Fe}}=3.384$ μ_B. The adsorption of the Fe atom induces an outward relaxation of the four nearest Pd neighbors by 0.06 Å and a magnetic moment of 0.26 μ_B on the nearest-neighbor Pd atoms. The induced magnetization is rather long ranged, and substantial magnetic moments are also found on the more distant Pd atoms (for details, see below), resulting in a giant effective moment of 7.64 μ_B/Fe atom.

The shortest distance between hollows on the Pd(001) surface is 2.794 Å; this is also the distance between two Fe atoms in an epitaxial Fe/Pd(001) monolayer. For a compact Fe/Pd(001) monolayer, the relaxed distance between an epitaxial Fe monolayer and the Pd surface is 1.704 Å, corresponding to a contraction of −13.7% compared to the interlayer distance in bulk Pd. The top layer of the Pd substrate relaxes outward by 4.5%; each Pd atom in the interface layer carries an induced magnetic moment of 0.34 μ_B. Together with a magnetic moment of 3.12 μ_B on each Fe atom and a weak magnetization of the Pd atoms also in the deeper layers, this gives an effective moment of 3.68 μ_B/Fe atom. The interlayer distance between the Fe monolayer at the substrate allows us to calculate the atomic volume of Fe in the layer. The value of 13.30 $Å^3$ is larger by 13.6% than the atomic volume in ferromagnetic bcc Fe—evidently, the expansion is a magnetovolume effect caused by the strongly increased magnetic moment, in agreement with our results for Fe/Rh(001) monolayers.[32] The predicted contraction of the Fe-Pd interlayer distance is larger than the experimental result of Lee *et al.*[47] obtained using low energy electron diffraction for a strongly intermixed film with nominal monolayer coverage, but in very good agreement with the theoretical results of this group for a compact Fe overlayer obtained using a full potential linearized plane-wave calcu-

lation in the generalized-gradient approximation.

The geometry of the supported Fe clusters on Pd(001) interpolates between the limits set by the isolated adatom and the compact monolayer, see Table I and Fig. 2. The Fe-Fe distances in the supported clusters are contracted compared to those in the epitaxial monolayer on average by about 0.1 Å, but these distances are still much larger than the interatomic distances in ferromagnetic bulk bcc Fe (2.45 Å), in an unsupported square Fe monolayer (2.33 Å) or in an Fe_2 dimer (1.81 Å).[40] In the supported Fe dimers and trimers, the contraction of the lateral Fe-Fe distances relative to the distance between the hollows in the surface is rather modest, only 0.06 Å, indicating that, in this case, the binding to the substrate dominates over the binding in the cluster. With increasing cluster size, the lateral contractions increase in a nonmonotonic way to up to 0.13 Å. The lateral contractions are largest for the rather compact clusters with four, six, or nine Fe atoms. The average distance between the Fe adatoms and the Pd surface increases from 1.33 Å for the monomer to 1.58 Å for the nine-atom cluster, but even in this cases, it is still smaller by 0.12 Å than for a monolayer and by 0.4 Å smaller than the interlayer distance in bulk Pd. For the clean Pd(001) surface, the relaxed distance between the two top layers is 1.952 Å, i.e., contracted by −1.2%. Adsorbed Fe atoms induce an outward relaxation of the Pd nearest neighbors, i.e., a buckling of the substrate. Likewise, the stronger bonding of the Fe atom at the rim of the cluster to the substrate leads to a buckling of the cluster. The largest buckling amplitudes of about 0.2 Å are calculated for the square Fe_9 cluster: the Pd atoms located below the center of the cluster show the largest outward relaxation, and the corners and edges of the cluster are bent toward the substrate.

The adsorption energy per Fe atom in the cluster [calculated relative to the clean Pd(001) surface and an Fe atom in bcc Fe] differs only modestly from that calculated for an Fe monolayer, indicating that the adsorption energy is determined mainly by the Fe-Pd interaction, while the lateral interaction between the cluster atoms is rather weak, see Fig. 2. Binding of monomers and dimers is slightly weaker than in a monolayer because of the lack of stabilizing Fe-Fe bonds; bonding in clusters with three to six Fe atoms is stronger compared to the monolayer because, as a consequence of the relaxation, the Fe-Fe bonds are less strained. In the nine-atom cluster, the energy of adsorption is already converged to the value in a complete overlayer. For an Fe_5 cluster, we have studied both a planar geometry and a tetragonal pyramid with the fifth atom in a second-layer position with a strongly reduced magnetic moment (see Fig. 1). The planar geometry is found to be lower in energy by 0.046 eV/Fe atom, although it has very low symmetry. Again, this emphasizes the dominant role of the Fe-Pd interaction.

B. Magnetic moments of cluster atoms

It is evident that both the average magnetic moments in the cluster and the magnetic moments induced on the substrate atoms depend on the cluster size. The largest magnetic moment (3.38 μ_B) is calculated for the isolated adatom; together with the magnetic moments induced on the Pd atoms,

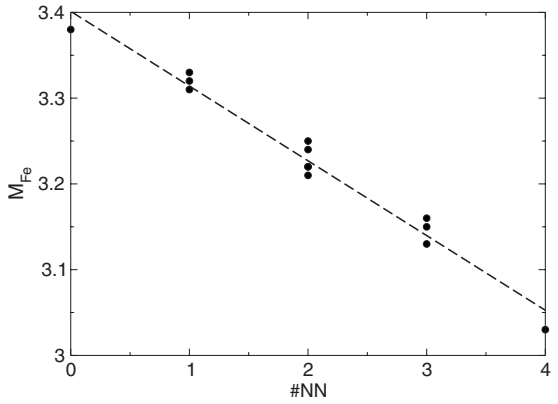

FIG. 3. Magnetic moments of Fe atoms in Fe_n/Pd(001) cluster with $n=1-6,9$ as a function of the number of Fe nearest neighbors (NN).

the effective magnetic moment is even 7.64 μ_B. In the nine-atom cluster, the average Fe moment is still 3.18 μ_B and the effective moment is 4.58 μ_B/Fe-atom. In the monolayer limit, the corresponding values are 3.12 and 3.68 μ_B; hence, the effective moments depend even more strongly on the cluster size.

In an unsupported square ferromagnetic monolayer of Fe, the equilibrium interatomic distance is 2.33 Å and the magnetic moment is 2.7 μ_B. If the interatomic distance is expanded to 2.80 Å to match the Pd(001) substrate, the magnetic moment is increased to 3.5 μ_B, which is slightly lower than the effective moment of the relaxed supported monolayer. This means that the reduction of the Fe moment through the hybridization with the substrate is overcompensated by the induced magnetization on the host atoms.

The decrease of the magnetic moments is usually attributed to an increased interaction between the 3*d* orbitals on neighboring atoms, which leads to more delocalized orbitals and hence a reduced tendency to magnetism. The same effect also influences the magnetic moments of the individual atoms in the cluster: sites with a larger number of Fe atoms have lower magnetic moments, irrespective of the shape of the cluster. This trend can be directly read from Fig. 3: sites with only one Fe neighbor (in clusters with 2, 3, or 5 atoms) have moments varying between 3.31 and 3.33 μ_B, sites with two Fe neighbors (in clusters with three, four, five, six, or nine atoms) have moments in the interval from 3.21 to 3.25 μ_B, and so on. Figure 3 shows that the variation of the local magnetic moment is almost strictly linear—a similar result has been reported by Mavropoulos *et al.*[26] for unrelaxed Fe clusters on the (001) and (111) surfaces of Ni and Cu.

The magnetic moments depend on the state of relaxation of the cluster, the relaxation in the vertical direction being more important than the lateral relaxation. For an isolated adatom on a nonrelaxed Pd(001) surface and in a site continuing the ideal fcc lattice of the substrate, we calculate a magnetic moment of 3.7 μ_B, to be compared with the value of 3.38 μ_B after full relaxation. For an Fe adatom in an unrelaxed position on Pd(001), the Green's-function calculations of Stepanyuk *et al.*[16] yield a magnetic moment of

3.5 μ_B, which is slightly lower than our result. The origin of the difference is in the use of the local density approximations, which always leads to a slightly lower magnetic moment than the generalized-gradient approximation used in our work. For a compact Fe monolayer continuing the ideal fcc geometry of the substrate, we calculate a magnetic moment of 3.42 μ_B, which is almost as large as the moment of a freestanding square Fe monolayer strained to the lattice constant of the Pd surface (3.5 μ_B). The influence on the effective moment is more modest, because the decrease of the Fe moments upon relaxation is largely counterbalanced by an increase of the induced moments on the Pd sites. The energy gain by the vertical relaxation is 0.15 eV/Fe atom, i.e., it accounts for about 40% of the total adsorption energy of the monolayer. The changes caused by a lateral relaxation are more modest. For example, for a five-atom cluster, we calculate the magnetic moments of 3.25/3.18/3.25/3.25/3.32 μ_B when only vertical relaxation is admitted, to be compared with the values of 3.21/3.16/3.21/3.22/3.33 μ_B for the fully relaxed cluster (cf. also Fig. 1). Hence, the average cluster moment is decreased by the full relaxation by 0.03 μ_B. The energy gain on lateral relaxation accounts for about 12% of the adsorption energy of the relaxed cluster.

C. Induced magnetization of the substrate: Giant effective moments

A very important aspect of ferromagnetic clusters supported on 4*d* substrates is the induced magnetic moments on the substrate atoms. Large magnetic moments on Pd or Pt atoms, induced by the covalent interaction with neighboring Fe atoms, have been reported before for dilute magnetic impurities,[6–8] for Pd/Fe/Pd trilayers, and for layered, $L1_0$-type intermetallic compounds.[48–50] The formation of induced magnetic moments is a very general phenomenon in nanostructured systems composed by magnetic 3*d* atoms and highly polarizable 4*d* or 5*d* elements, see, e.g., Ref. 28 and further references compiled therein. For the Fe_n/Pd(001) clusters, the contribution of the induced moments to the total cluster moment per Fe atom decreases from 4.64 μ_B for the isolated adatom to 0.56 μ_B for the compact monolayer. The magnitude of the effective moments for the smallest clusters is in good agreement with earlier results on Fe impurities in bulk Pd.[6–8]

The largest induced magnetic moments are found on the Pd atoms binding to atoms of the cluster; they depend strongly on the number of Fe neighbors, see Fig. 4: for a Pd atom with only one Fe nearest neighbor, it varies between 0.26 μ_B for the adatom and 0.17 μ_B for an atom next to the corner atom of a larger cluster. The largest induced moment of 0.41 μ_B is calculated for the Pd atom just below the center of a four-atom cluster. The induced moment for four-coordinated Pd atoms decreases slightly for larger clusters, reaching 0.34 μ_B for the Pd-interface atoms facing a compact Fe monolayer. Green's-function calculations by Stepanyuk *et al.*[16] for an Fe adatom and monolayers in unrelaxed positions above the Pd(001) surface yield induced moments on Pd nearest-neighbor sites of 0.14 μ_B for the adatom and 0.33 μ_B for the monolayer, illustrating the strong influence of the inward relaxation of the magnetic adatom on the induced moment.

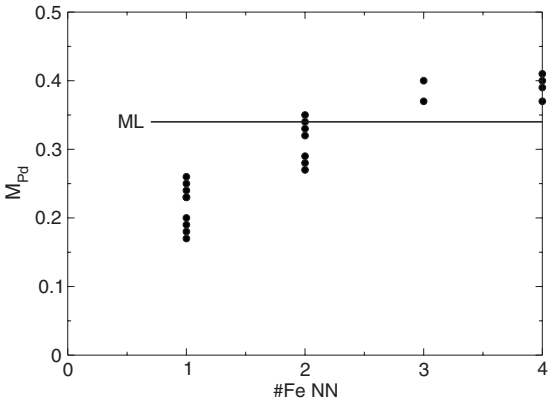

FIG. 4. Induced magnetic moments (in μ_B) of Pd atoms in Fe_n/Pd(001) clusters with $n=1-6,9$ as a function of the number of Fe neighbors. The horizontal line marks the magnetic moment of Pd atoms in contact with an Fe monolayer.

Substantial magnetic moments are also induced on the more distant Pd atoms. Figure 5 shows the distribution of the moments induced by an isolated Fe adatom on the atoms of the three top layers of the substrate. The induced magnetization cloud extends to the boundaries of the surface cell and to the deepest layer of our model. About 41% of the induced magnetization is located in the top layer, and 27% and 20% in the first and second subsurface layers. This distribution of the induced magnetization is almost independent of the cluster size; similar values apply even to a full adsorbed Fe monolayer. For the larger clusters, the overlap of the magnetization clouds induced by the periodically repeated cluster becomes, of course, substantial—one has to remember that a nine-atom cluster in a 5×5 supercell represents a coverage of 0.36 monolayers.

The variation of the induced moments as a function of the distance from the central atom in the Fe_n cluster is analyzed in Fig. 6 for $n=1$ and $n=9$. For the isolated adatom, the induced magnetic moments decrease approximately with the square of the distance from the adatom. For the nine-atom cluster, the moments induced on the Pd atoms just below the cluster are almost equal to the moments induced by an Fe monolayer. At the boundary of the supercell, the induced moments on the top Pd layer are strongly decreased, whereas the effect of the neighboring cluster is more pronounced in the subsurface layer. Hence, the effective moments given here should not be considered as quantitatively reliable for an isolated cluster.

The induced moments depend also on the state of relaxation of the cluster. As discussed above, vertical relaxation leads to an increase of the induced moment counterbalancing the decrease of the cluster moments. Interestingly, a full three-dimensional relaxation leads to a slight reduction of the moments on the Pd atoms close to the outer rim of the cluster (by 0.02–0.03 μ_B) because the contraction of the Fe-Fe distances leads to an increase of the Fe-Pd distances.

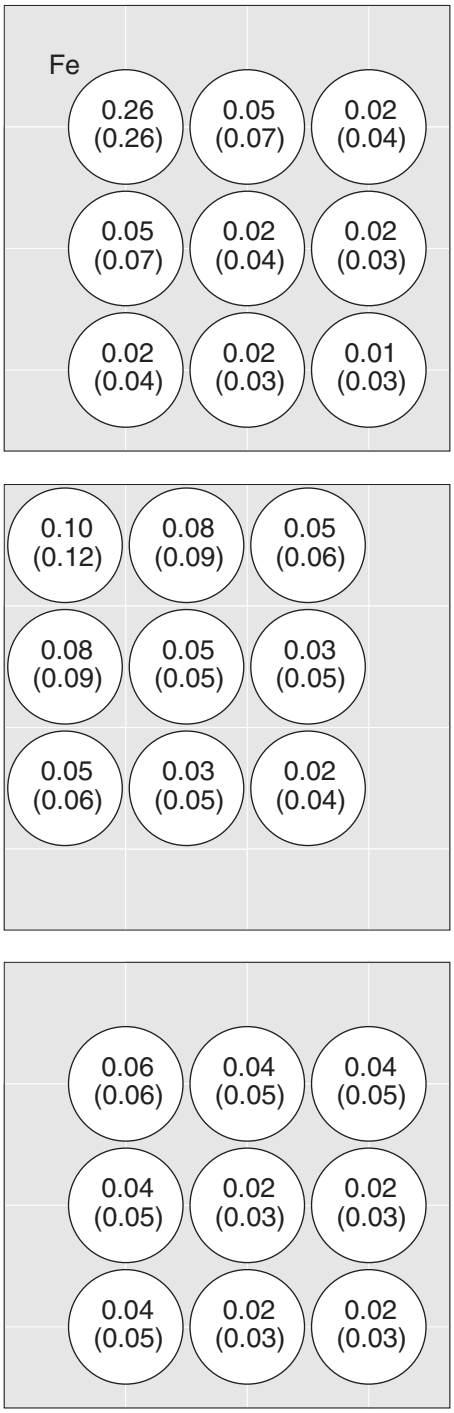

FIG. 5. Magnetic spin moments (in μ_B) induced by an isolated Fe adatom on the Pd atoms in the first to third substrate layers (top to bottom). Numbers in parentheses show the spin moments derived from fully relativistic calculations including spin-orbit coupling.

D. Orbital magnetic moments

It has been claimed that in small clusters of magnetic atoms, orbital moments are strongly enhanced compared to the spin moment. However, for gas-phase clusters, the existing calculations based on semiempirical tight-binding methods[51,52] predict widely differing values. Fully relativistic

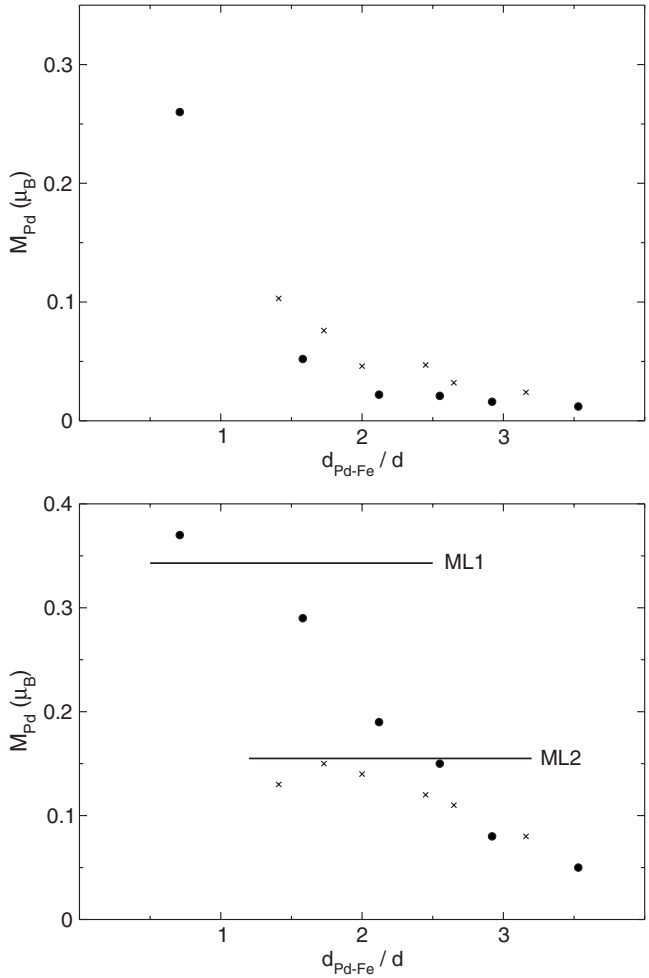

FIG. 6. Magnetic moments on the Pd atoms in the surface (full dots) and subsurface (crosses) layers induced by a single Fe adatom (top) and by a nine-atom Fe cluster (bottom), plotted as a function of the distance from the central Fe atom. Distances are normalized by the distance d between Pd atoms in the surface layer. The horizontal lines show, for comparison, the moments of Pd atoms in the first and second layers induced by a compact Fe adlayer (cf. text).

Green's-functions KKR calculations of Lazarovits *et al.*[22] for Fe and Co clusters on Ag(001) predict orbital moments of M_L=0.88 μ_B for an isolated Fe adatom and M_L=1.19 μ_B for Co, decreasing rapidly with increasing size of the cluster. Sipr *et al.*[27] find M_L=1.0 μ_B for a Co atom on Au(111), but only M_L=0.64 μ_B on Pt(111). For adsorbed clusters, the work of Pick *et al.*[24] has demonstrated that the relaxation of the cluster geometry influences orbital moments even more than spin moments. For an isolated Co adatom on a Cu(001) surface, an inward relaxation of 0.24 Å induces a reduction of the orbital moment by 27%. Anisotropies of orbital moments and anisotropy energies have been calculated using the self-consistent potentials for a perpendicular magnetic moment and the magnetic force theorem. For Fe atoms and clusters, in-plane orbital moments are always lower than for perpendicular orientation, whereas for Co and Ni, the anisotropy can have either sign.[22] The anisotropy of the orbital moments also determines the magnetic anisotropy energy according to perturbation theory.[53]

TABLE II. Spin, orbital, and total magnetic moments (in μ_B) of an Fe adatom on a Pd(001) substrate and induced moments on the Pd-substrate atoms (integrated over all atoms in the supercell). Results for perpendicular and in-plane orientations of the magnetic moment are presented. For the spin moments, the results obtained without spin-orbit coupling are given in parentheses.

	Spin	Orbital	Total
	Perpendicular		
M_{Fe}	3.38 (3.38)	0.073	3.45
M_{Pd}	4.52 (4.26)	0.574	5.09
Effective moment	7.90 (7.64)	0.674	8.54
	In plane		
M_{Fe}	3.38	0.082	3.46
M_{Pd}	1.40	0.150	1.55
Effective moment	4.78	0.232	5.01

Here, we present a fully relativistic self-consistent calculation for an Fe adatom on Pd(001). We have performed two sets of self-consistent calculations: one with the spin moment initially oriented perpendicular to the surface and one with an in-plane orientation. Our approach allows for an independent reorientation of both the spin and orbital moments, but we find that spin and orbital moments remain collinear (although not necessarily parallel). The calculations have been performed for the geometry resulting from the scalar relativistic calculations. We have verified that the forces acting on the atoms are sufficiently small so that a change in the geometry induced by relativistic effects can be excluded. Our results are compiled in Table II.

The main results are as follows: (i) The orbital moments of the Fe adatoms are parallel to the spin moment and remain very modest, $M_L \sim 0.07\ \mu_B$ for perpendicular and $M_L \sim 0.08\ \mu_B$ for in-plane orientation. This is a consequence of the massive inward relaxation by 0.65 Å leading to the strong hybridization of the Fe 3*d* orbitals with the 4*d* orbitals of the substrate, which quenches the orbital moments almost as efficiently as in bulk Fe. (ii) Substantial orbital moments are induced on the substrate atoms; they differ strongly for perpendicular and in-plane orientations. (iii) Spin-orbit coupling also influences the orientation and size of the induced spin moments (see Fig. 5). (iv) The strong orientation dependence of the induced moments enhances the magnetic anisotropy—we find perpendicular orientation to be preferred by 32 meV.

We will discuss first the simpler cases of perpendicular magnetization. For the Fe adatom, the orbital moment is only about 2% of the spin moment. On the Pd surface atoms that are nearest neighbors to the Fe atom, the induced spin and orbital moments are 0.262 and 0.032 μ_B, respectively, corresponding to a ratio $M_L/M_s=0.13$. On the Pd atom in the subsurface layer immediately below the Fe atom, the spin and orbital moments are 0.12 and 0.022 μ_B. Small orbital moments are also found on the more distant Pd atoms, adding up to an effective orbital moment of 0.67 μ_B and a ratio of $M_L^{\mathrm{eff}}/M_S^{\mathrm{eff}}=0.078$. All induced spin and orbital moments are parallel to the magnetic moment of the Fe atom; the distribution of the local spin and orbital moments reflects the fourfold symmetry around the *z* axis perpendicular to the Pd surface.

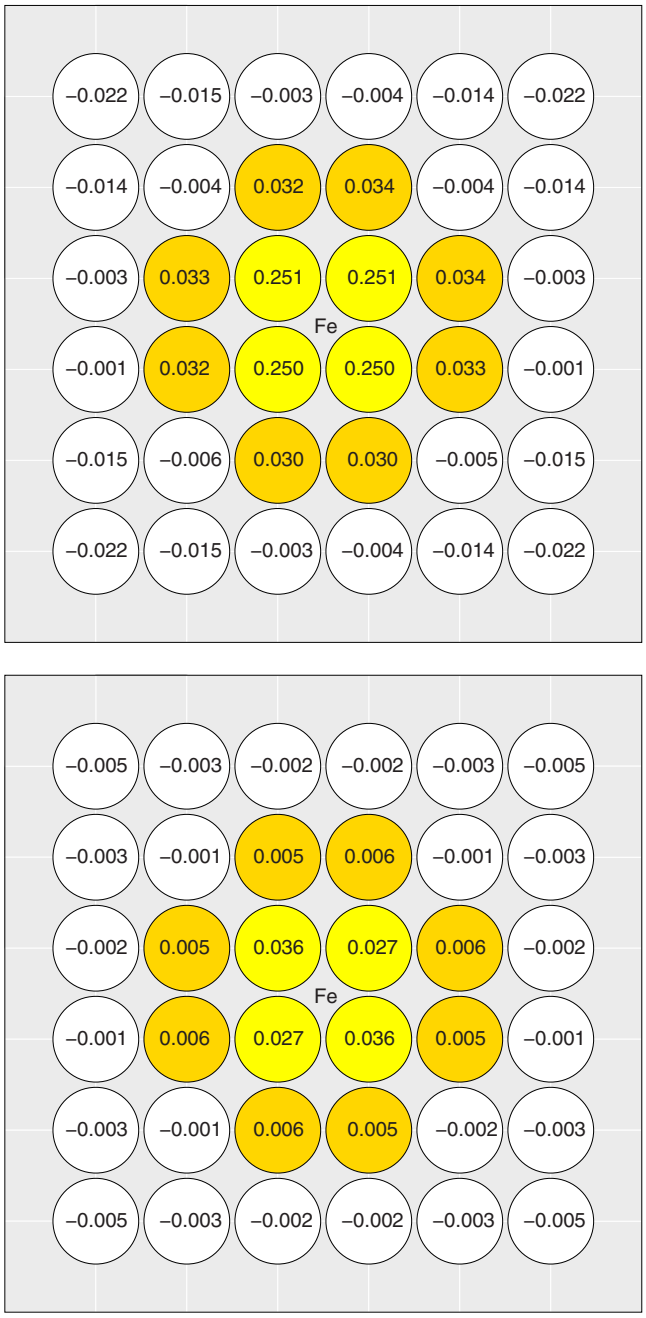

FIG. 7. (Color online) Magnetic spin (top) and orbital (bottom) moments on the Pd atoms in the surface layer induced by a single Fe adatom with an in-plane orientation of the magnetic moment (cf. text).

An in-plane orientation of the magnetic moment on the Fe atom (along the *x* axis) reduces the symmetry from fourfold to twofold (from C_{4v} to C_{2v}). In addition, the induced spin and orbital magnetic moments can now be oriented antiparallel to the Fe moment; as an example, we show in Fig. 7 the distribution of the induced spin and orbital moments in the Pd surface layer. Compared to a perpendicular magnetic mo-

ment, the orbital moments of the Fe atom are slightly enhanced. The induced spin moments on the nearest-neighbor Pd atoms are only slightly reduced (from 0.26 to 0.25 μ_B), but already for next-nearest neighbors, the induced moments are reduced to 50%, and on the more distant sites, the induced moments are even antiparallel to the Fe moment. The same observation holds for the induced orbital moments for which the symmetry breaking is even more evident. For a perpendicular orientation, the induced orbital moments on the nearest-neighbor sites are 0.032 μ_B; for in-plane orientation, two Pd atoms carry an orbital moment of 0.036 μ_B and another two carry a moment of 0.027 μ_B. A tendency to form antiparallel induced moments is also found in the deeper layer. For perpendicular orientation, the integrated induced spin moments are 2.07/1.42/1.03 μ_B for the three top layers; for in-plane orientation, the corresponding values are 1.17/0.26/−0.01 μ_B. For the orbital moments, we find 0.25/0.18/0.14 μ_B for perpendicular and 0.14/0.02/−0.01 μ_B for in-plane orientation. Hence, while for the adatom the spin moment shows no anisotropy and the orbital moment only a modest anisotropy, both the induced spin and orbital moments are strongly anisotropic.

The strong anisotropy of the induced moments also explains the unusually large value of the magnetic anisotropy energy (MAE). According to Bruno[53] and van der Laan,[54] the anisotropy energy is proportional to the strength of the spin-orbit coupling and the anisotropy of the orbital moment (assuming that the spin moment is unchanged upon reorientation). This simplified analysis shows that because of both the larger anisotropy of the induced orbital moment and the stronger spin-orbit coupling in Pd, the contribution of the Pd-interface atoms dominates the MAE. Similarly large values of the MAE have been reported by Nonas *et al.*[21,55] for isolated adatoms on Ag(001), but only if a heuristic orbital polarization term[56] is added to the Hamiltonian, leading to a very strong enhancement of the orbital moment of the 3*d* adatom (any contribution from the induced moments being neglected). However, in their second paper,[55] Cabria *et al.* give a rather critical assessment of the orbital polarization mechanism, pointing out that for Fe impurities in Ag, the DFT predictions for the local moment and the hyperfine field are in good agreement with experiment, while the orbital polarization scheme leads to wrong result. Our study suggests that the induced orbital moments neglected in all previous studies play an important role in determining the MAE.

E. Electronic structure and magnetism

The physical mechanism determining the variation of the local magnetic moments in nanostructures has been discussed by Dennler *et al.*[28] within the framework of the theory of itinerant magnetism, following earlier arguments based on observations by photoelectron spectroscopy[57] and DFT calculations.[58,59] Larger local magnetic moments correlate with a larger exchange splitting. The constant of proportionality is the Stoner parameter I; the fact that $I \sim 1$ eV/μ_B is independent of the local arrangement shows that it may be identified with the Hund's rule exchange parameter J. We illustrate this only very briefly in terms of an analysis of the spin-polarized electronic density of states (DOS). Figure 8(a) compares the local DOS of an isolated Fe adatom with that of a compact Fe monolayer. For the adatom, the majority states are completely occupied; the part of the DOS between −3 eV and the Fermi energy is due to the hybridization with the Pd 4*d* band. The dominant feature of the minority DOS is the very narrow peak just above E_F. For the monolayer, the width of the majority band is unchanged, but due to the increased hybridization, the center of gravity is shifted to lower binding energies. In the minority DOS, the lateral Fe-Fe interaction leads to a bonding-antibonding splitting. If the exchange splitting is evaluated in terms of the center of gravity of spin-up and spin-down bands, a Stoner parameter of $I = \sim 1 \pm 0.1$ eV/μ_B is obtained. The Stoner picture applies even to the more subtle differences in the magnetism of the center, edge, and corner atoms of the nine-atom cluster, see Fig. 8(b). The larger magnetic moments of the corner atoms parallel a larger exchange-splitting (which is due to the downshift of the center of gravity of the majority DOS). The local values of the Stoner parameter fall within the limits given above.

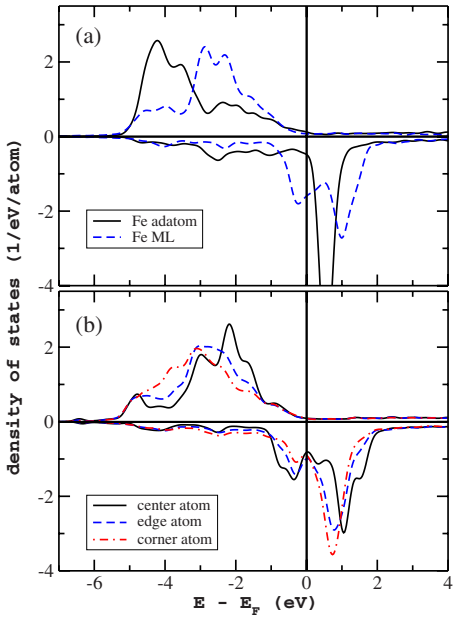

FIG. 8. (Color online) (a) Spin-polarized electronic density of states (DOS) for an isolated Fe adatom and for a compact Fe monolayer on Pd(001). (b) Local spin-polarized electronic DOS for center, edge, and corner atoms in an Fe_9/Pd(001) cluster (cf. text).

IV. CONCLUSIONS

We have used *ab-initio* DFT calculations to study the morphology and magnetism of Fe_n clusters supported on Pd(001). For the cluster sizes considered in our investigations, the Fe atoms form slightly buckled two-dimensional islands on the substrate. As a result of the size mismatch between Fe and Pd, the geometry of the clusters does not simply propagate the crystal structure of the substrate. The most important effect is a strong inward relaxation of the Fe

atoms compared to the interlayer distance in bulk Pd, by 0.65 Å for an isolated adatom and by 0.40 Å for an Fe_9 cluster. In addition to the vertical relaxation, a modest contraction of the lateral distances between the Fe atoms and a buckling of both cluster and substrate is calculated.

The magnetic moments of Fe atoms in the cluster are strongly enhanced compared to bulk Fe, and even in the largest nine-atom cluster, they are still larger than in a compact Fe/Pd(001) monolayer. The total cluster moments are further enhanced by the induced magnetization of Pd atoms in the vicinity of the adsorbed cluster; for all clusters considered here, the effective magnetic moment per Fe atom is larger than the limiting value of the spin moment of an isolated Fe atom set by Hund's rule, i.e., $\geqslant 4\ \mu_B$. The giant effective moments calculated for the smallest clusters are of the same magnitude as the effective moments of Fe impurities bulk Pd.[6–8] The size dependence of the average cluster moments is a consequence of the increasing average Fe-Fe coordination number. The local magnetic moment of an Fe atom in the cluster depends only on the local coordination number and is independent of the size and shape of the cluster, following a linear relation between coordination and spin moment. The local induced moments on the Pd atoms depend on the number of nearest-neighbor Fe atoms. The size dependence of the effective moment per Fe atom is even more pronounced than that of the cluster moments. The relaxation of the cluster structure influences the magnetic moments in the cluster and induced in the substrate in opposite directions: Fe moments are reduced upon relaxation because of the enhanced Fe-Pd (and if lateral relaxation is permitted, also Fe-Fe) hybridization. On the other hand, a closer Fe-Pd interaction leads to an increase of the induced moments.

For an isolated Fe adatom on Pd(001), we have performed self-consistent fully relativistic calculations including spin-orbit coupling for perpendicular and in-plane orientations of the magnetic moment. We find that for the adatom in a relaxed position, the enhancement of the orbital moment over the bulk value is only very modest. On the other hand, for the induced moments on the substrate atoms, a much larger value of the ratio M_L/M_S between orbital and spin moments is found. For a perpendicular orientation of the moments, the induced orbital moments make a non-negligible contribution to the effective moment. Spin-orbit coupling leads to a pronounced anisotropy of the induced moment: for an in-plane orientation, not only the orbital but also the spin-moments induced in the substrate are strongly reduced. The strong anisotropy of the induced moments leads to a large magnetic anisotropy energy dominated by contributions from the Pd-interface atoms. These results, although for reasons of the high computational effort restricted to the case of an isolated adatom, shed light on the magnetic properties of clusters supported on highly polarizable metallic substrates. Future work will extend the relativistic calculations to larger supported clusters.

ACKNOWLEDGMENTS

This work has been supported by Project "Software Lizenzen VASP" FA 513 901. The assistance of Michal Jahnatek in data analysis and computer graphics is gratefully acknowledged.

*juergen.hafner@univie.ac.at

[1] W. A. de Heer, P. Milani, and A. Châtelain, Phys. Rev. Lett. **65**, 488 (1990).
[2] I. M. Billas, A. Châtelain, and W. A. de Heer, Science **265**, 16581 (1994).
[3] J. T. Lau, A. Föhlisch, R. Nietubyc, M. Reif, and W. Wurth, Phys. Rev. Lett. **89**, 057201 (2002).
[4] P. Gambardella, S. Rusponi, M. Veronese, S. S. Dhesi, C. Garzioli, A. Dallmeyer, I. Cabria, R. Zeller, P. H. Dederichs, K. Kern, C. Carbone, and H. Brune, Science **300**, 1130 (2003).
[5] G. G. Low and T. M. Holden, Proc. Phys. Soc. London **89**, 119 (1966).
[6] T. Herrmannsdörfer, S. Rehmann, W. Wendler, and F. Pobell, J. Low Temp. Phys. **104**, 49 (1996).
[7] K. Swieca, Y. Kondo, and F. Pobell, Phys. Rev. B **56**, 6066 (1997).
[8] B. H. Verbeek, G. J. Nieuwenhuys, J. A. Mydosh, C. van Dijk, and B. D. Rainford, Phys. Rev. B **22**, 5426 (1980).
[9] M. Ulmeanu, C. Antoniak, U. Wiedwald, M. Farle, Z. Frait, and S. Sun, Phys. Rev. B **69**, 054417 (2004).
[10] C. Antoniak, J. Lindner, M. Spasova, D. Sudfeld, M. Acet, M. Farle, K. Fauth, U. Wiedwald, H. G. Boyen, P. Ziemann, F. Wilhelm, A. Rogalev, and S. Sun, Phys. Rev. Lett. **97**, 117201 (2006).
[11] R. Félix-Medina, J. Dorantes-Dávila, and G. M. Pastor, Phys. Rev. B **67**, 094430 (2003).
[12] R. Robles, R. C. Longo, E. G. Noya, A. Vega, and L. J. Gallego, Phys. Rev. B **69**, 115427 (2004).
[13] E. Martinez, R. C. Longo, R. Robles, A. Vega, and L. J. Gallego, Phys. Rev. B **71**, 165425 (2005).
[14] G. Nicolas, J. Dorantes-Dávila, and G. M. Pastor, Phys. Rev. B **74**, 014415 (2006).
[15] R. C. Longo, E. Martinez, O. Dieguez, A. Vega, and L. J. Gallego, Nanotechnology **18**, 055701 (2007).
[16] V. S. Stepanyuk, W. Hergert, K. Wildberger, R. Zeller, and P. H. Dederichs, Phys. Rev. B **53**, 2121 (1996).
[17] V. S. Stepanyuk, W. Hergert, P. Rennert, K. Wildberger, R. Zeller, and P. H. Dederichs, J. Magn. Magn. Mater. **165**, 272 (1997).
[18] V. S. Stepanyuk, W. Hergert, P. Rennert, K. Kokko, A. F. Tatarchenko, and K. Wildberger, Phys. Rev. B **57**, 15585 (1998).
[19] V. S. Stepanyuk, W. Hergert, P. Rennert, J. Izquierdo, A. Vega, and L. C. Balbás, Phys. Rev. B **57**, R14020 (1998).
[20] D. I. Bazhanov, W. Hergert, V. S. Stepanyuk, A. A. Katsnelson, P. Rennert, K. Kokko, and C. Demangeat, Phys. Rev. B **62**, 6415 (2000).
[21] B. Nonas, I. Cabria, R. Zeller, P. H. Dederichs, T. Huhne, and H. Ebert, Phys. Rev. Lett. **86**, 2146 (2001).
[22] B. Lazarovits, L. Szunyogh, and P. Weinberger, Phys. Rev. B **65**,

104441 (2002).
[23] S. Pick, V. S. Stepanyuk, A. N. Baranov, W. Hergert, and P. Bruno, Phys. Rev. B **68**, 104410 (2003).
[24] S. Pick, V. S. Stepanyuk, A. L. Klavsyuk, L. Niebergall, W. Hergert, J. Kirschner, and P. Bruno, Phys. Rev. B **70**, 224419 (2004).
[25] H. Ebert, S. Bornemann, J. Minar, P. H. Dederichs, R. Zeller, and I. Cabria, Comput. Mater. Sci. **35**, 279 (2005).
[26] P. Mavropoulos, S. Lounis, R. Zeller, and S. Blügel, Appl. Phys. A: Mater. Sci. Process. **82**, 103 (2006).
[27] O. Šipr, S. Bornemann, J. Minár, S. Polesya, V. Popescu, A. Šimunek, and H. Ebert, J. Phys.: Condens. Matter **19**, 096203 (2007).
[28] S. Dennler, J. Hafner, M. Marsman, and J. Morillo, Phys. Rev. B **71**, 094433 (2005).
[29] D. Spišák and J. Hafner, Phys. Rev. B **66**, 052417 (2002).
[30] D. Spišák and J. Hafner, Phys. Rev. B **67**, 214416 (2003); Comput. Mater. Sci. **30**, 278 (2004).
[31] D. Spišák and J. Hafner, Phys. Rev. B **70**, 014430 (2004).
[32] D. Spišák and J. Hafner, Phys. Rev. B **73**, 155428 (2006).
[33] G. Kresse and J. Furthmüller, Phys. Rev. B **54**, 11169 (1996); Comput. Mater. Sci. **6**, 15 (1996).
[34] P. E. Blöchl, Phys. Rev. B **50**, 17953 (1994).
[35] G. Kresse and D. Joubert, Phys. Rev. B **59**, 1758 (1999).
[36] D. Hobbs, G. Kresse, and J. Hafner, Phys. Rev. B **62**, 11556 (2000).
[37] M. Marsman and J. Hafner, Phys. Rev. B **66**, 224409 (2002).
[38] J. P. Perdew, K. Burke, and K. Ernzerhof, Phys. Rev. Lett. **77**, 3865 (1996).
[39] S. H. Vosko, L. Wilk, and M. Nusair, Can. J. Phys. **58**, 1200 (1980).
[40] E. G. Moroni, G. Kresse, J. Hafner, and J. Furthmüller, Phys. Rev. B **56**, 15629 (1997).
[41] P. Villars and L. D. Calvert, *Pearson's Handbook of Crystallographic Data for Intermetallic Phases*, 2nd ed. (American Society for Metals, Metals Park, OH, 1991).
[42] M. Methfessel and A. T. Paxton, Phys. Rev. B **40**, 3616 (1989).
[43] C. Liu and S. D. Bader, Phys. Rev. B **44**, 2205 (1991).
[44] K. J. Strandbrug, D. W. Hall, C. Liu, and S. D. Bader, Phys. Rev. B **46**, 10818 (1992).
[45] X. F. Jin, J. Barthel, J. Shen, S. S. Manoharan, and J. Kirschner, Phys. Rev. B **60**, 11809 (1999).
[46] C. Boeglin, H. Bulou, J. Hommet, X. Le Cann, H. Magnan, P. LeFevre, and D. Chandesris, Phys. Rev. B **60**, 4220 (1999).
[47] S. K. Lee, J. S. Kim, B. Kim, Y. Cha, W. K. Han, H. G. Min, J. Seo, and S. C. Hong, Phys. Rev. B **65**, 014423 (2001).
[48] S. Mitani, K. Takanashi, M. Sano, H. Fujimori, A. Osawa, and H. Nakajima, J. Magn. Magn. Mater. **148**, 163 (1995).
[49] E. Holmström, L. Nordström, and A. M. N. Niklasson, Phys. Rev. B **67**, 184403 (2003).
[50] A. B. Shick and O. N. Mryasov, Phys. Rev. B **67**, 172407 (2003).
[51] R. A. Guirado-Lopez, J. Dorantes-Davila, and G. M. Pastor, Phys. Rev. Lett. **90**, 226402 (2003).
[52] X. Wan, L. Zhou, J. Dong, T. L. Lee, and D. Wang, Phys. Rev. B **69**, 174414 (2004).
[53] P. Bruno, Phys. Rev. B **39**, 865 (1989).
[54] G. van der Laan, J. Phys.: Condens. Matter **10**, 3239 (1998).
[55] I. Cabria, B. Nonas, R. Zeller, and P. H. Dederichs, Phys. Rev. B **65**, 054414 (2002).
[56] M. S. S. Brooks, Physica B **130**, 6 (1985).
[57] F. J. Himpsel, Phys. Rev. Lett. **67**, 2363 (1991).
[58] I. Turek, Ch. Becker, and J. Hafner, J. Phys.: Condens. Matter **4**, 7257 (1992).
[59] Ch. Becker and J. Hafner, Phys. Rev. B **50**, 3913 (1994).